Westerduinweg 3
1755 LE Petten
P.O. Box 15
1755 ZG Petten
The Netherlands

www.tno.nl

T +31 88 866 50 65

TNO report

TNO 2019 R11982 | Final report revision 1

Scanning LiDAR measurements in Rotterdam harbour

Date	15 Januari 2020
Author(s)	C. Stock-Williams, E.K. Fritz, J.W. Wagenaar, G. Bergman
Copy no	
No. of copies	
Number of pages	23 (incl. appendices)
Number of appendices	
Sponsor	
Project name	MIIP Windlass pilot
Project number	060.39123

Contents

Management Summary

MARIN (project lead), ECN.TNO and TU Eindhoven have jointly set-up the 'Wind Loads And Securing Ships' (WINDLASS) pilot project, where a scanning LiDAR was installed in the Rotterdam harbour. The project aims to demonstrate the scanning LiDAR and to assess the 3D wind field. Specifically, this project has three goals:

- Assess the scanning LiDAR in terms of how it compares to a meteorological mast and how it deals with surrounding obstacles as masts and possibly cranes.
- Assess incoming wind fields from the sea to the land and towards a large state of the art wind turbine.
- Develop a wind field reconstruction algorithm to provide reliable 3D wind fields from the measured radial wind speeds of the scanning LiDAR system.

The validation results of the scanning LiDAR through the wind speed reconstruction algorithm with the meteorological mast for 10-minute average wind speeds showed a bias of +0.27 m/s and a high standard deviation of 1.32 m/s.

With respect to how the wind approaches from sea to land in the free stream (undisturbed wind conditions), no clear conclusions can be drawn. Nevertheless, the study clearly shows that terrain influences are still visible at 100m relevant for undisturbed wind condition assumptions in for instance power performance testing. However, at this moment there is no indication that influences are such that undisturbed wind condition assumptions need to be revised.

With respect to the wind field reconstructed flow fields around and in between container ships, the effects of the tall structures can be clearly seen in the results: wake in the lee of the containers at higher heights; speed-up effects and turbulence around containers at low heights; and an alignment of the flow with the pathways running through the containers.

1 Introduction

Wind is a very complex phenomenon as it is 3-dimensional and potentially very dynamic. It comprises the abstract concept of turbulence, where energy is dissipated in a cascade breakdown from large eddies to smaller and smaller eddies. This complex wind phenomenon has very different viewpoints and/or application areas: among others as the resource for wind energy; the transport medium for aeroplanes; and influencing factor in large shipping.

Research institutes, among which ECN (now TNO and further referred to as ECN.TNO) and MARIN, have recognized the common denominator in these application areas and value the collaborative research in the 3-dimensional wind field using scanning LiDAR measurement technology. Together, they have set-up WindScanner.nl [1] and, simultaneously, ECN purchased a long range scanning LiDAR (Leosphere WindCube 200S [2]) end of 2017. Such a scanning LiDAR shoots laser pulses into the air and, from the back-scattered Doppler shifted pulses, determines the radial wind speed, i.e. the wind speed resolved along the beam. Ranges from 100m to 7km are possible.

One of ECN.TNO's interests in detailed wind fields is the transition from sea to shore. Wind fields generally travel quite smoothly over sea, yet, over land they are influenced by the surface roughness and temperature reflections causing turbulence and vertical mixing, respectively. This is important for wind energy development in such areas and particularly for the GE Haliade X prototype wind turbine, erected in the harbour of Rotterdam Maasvlakte [3].

In addition, MARIN's interest is that harbours are placed more and more offshore, as for instance Rotterdam's Maasvlakte 2, where wind speeds are much higher. At the same time container ships are becoming larger and high wind speeds strongly influence the mooring to the quay side of such large ships. Hence, detailed understanding of wind fields in the harbour is of utmost importance.

Besides these applications, there is the interest to enhance the capabilities of LiDAR measurements using software. Here, a machine learning-based wind field reconstruction algorithm is being developed, which extrapolates the wind information in space and time, beyond where is actually measured, using so-called Gaussian Processes. This will enable to reconstruct entire wind fields from a single scanning LiDAR. The first step of this development was made in [4] using ground-based static LiDAR profilers and in [5] the algorithm was tested on scanning LiDAR measurements.

These interests are joined in the pilot project 'Wind Loads And Securing Ships' (WINDLASS) setup by MARIN (project lead), ECN.TNO and TU Eindhoven with subsidy from the 'Maritieme Innovatie-Impuls Projecten' (MIIP) framework organised by the Innovation Council of 'Nederland Maritiem Land' [6], where the ECN.TNO scope was defined in [7]. In short, the aim is to demonstrate the scanning LiDAR and to assess the 3D wind field. Specifically, this project has three goals:

- Assess the scanning LiDAR in terms of how it compares to a meteorological mast and how it deals with surrounding obstacles as masts and possibly cranes.

- Assess incoming wind fields from the sea to the land and towards a large state of the art wind turbine.
- Develop a wind field reconstruction algorithm to provide reliable 3D wind fields from the measured radial wind speeds of the scanning LiDAR system.

This report describes the findings of ECN.TNO's part of project, focusing on the goals described above. Consequently, chapter 2 describes the test environment set-up with the details on the positions of the instruments, the layout of the meteorological mast and the programmed scan patterns of the LiDAR. Next, the validation of the reconstructed wind speeds with the meteorological mast is described in chapter 3. Last, findings from the wind field velocity reconstruction are presented in chapter 4 and this report closes with conclusions and recommendations in chapter 5.

2 Test Environment

2.1 Location

At the SIF Group – a leading company in offshore support structures - site in Rotterdam Maasvlakte a Windcube WLS-200S scanning LiDAR (WLS-200S) is installed in September 2019 in between the meteorological mast and the turbine location, see Figure 1 and Figure 2. From this location the LiDAR has a clear view towards the meteorological mast, towards the sea and towards the container terminals.

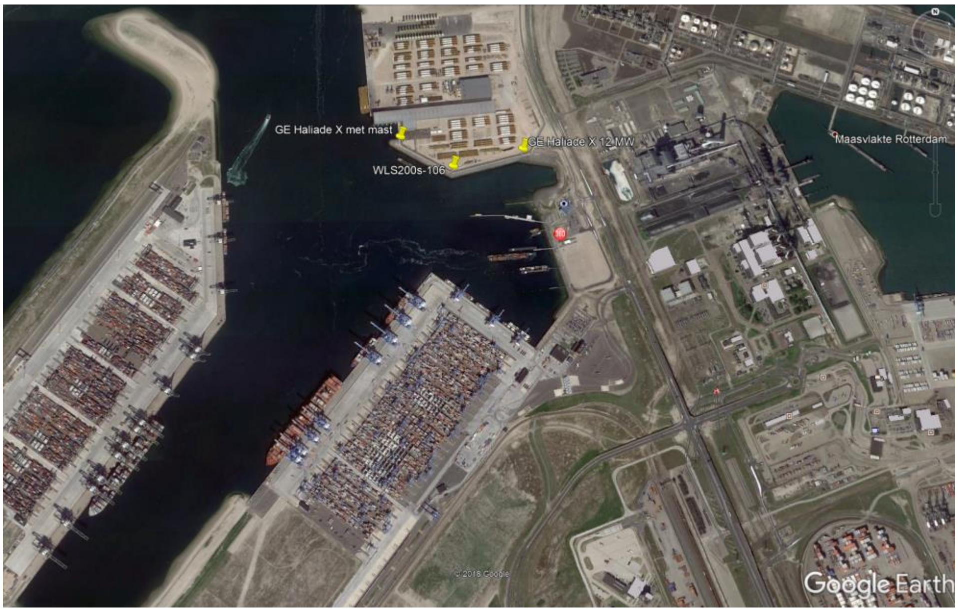

Figure 1 Overview of the surrounding of the SIF site in Rotterdam Maasvlakte

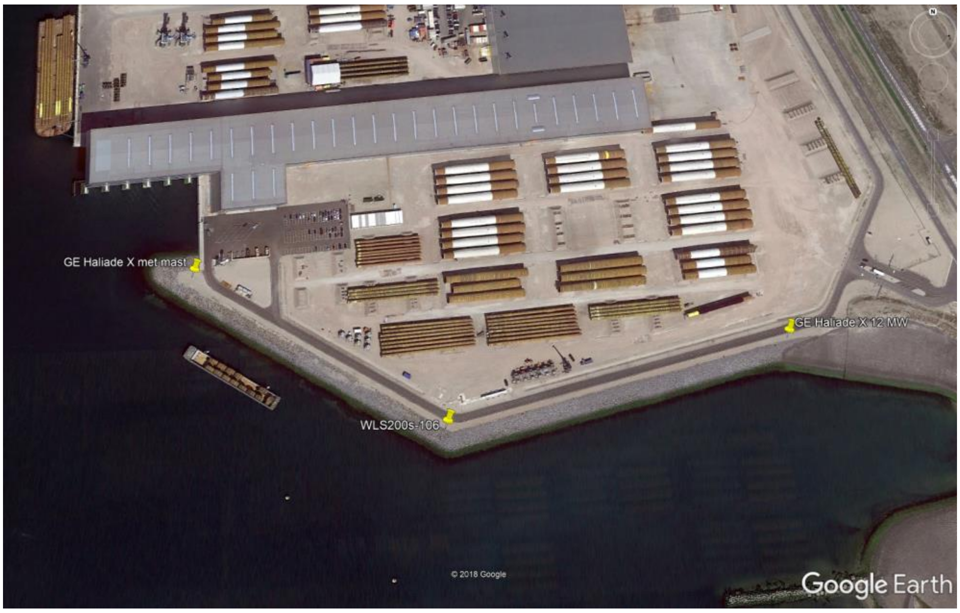

Figure 2 LiDAR, meteorological mast and turbine locations at SIF site in Rotterdam Maasvlakte

2.2 Windcube WLS-200S scanning LiDAR

For the WINDLASS pilot project the scanning LiDAR of ECN.TNO is used, see Figure 3. This is a doppler LiDAR system for high precision radial wind speed measurements up to a range of ~7km, to be configured in different scan patterns.

Figure 3 Windcube WLS-200S at the SIF site

The scanning LiDAR has the ability of executing four scan patterns, being [2]:
PPI, horizontal scanning pattern
RHI, vertical scanning pattern
DBS, this is a scanning mode for wind resource assessment, comparable to the ground based LiDAR, to measure wind speed and wind direction at different heights simultaneously.
Fixed, continuous scan at a fixed azimuth angle and elevation angle.

For the WINDLASS pilot measurement campaign the PPI and RHI scanning patterns are used.

The GPS location of the WLS-200s is (LAT 51.961843°, LON 4.008462°)

2.3 Meteorological mast

The meteorological mast installed on the SIF site is used for validation of the WLS-200S scanning LiDAR. For the validation scans 3 elevations are configured to meet the 3 measurement heights of the mast: 25m, 80m and 135m (see Figure 4). Apart from the cup anemometers, which measure the horizontal wind speed at the 3 levels, also sonic anemometers are installed at 21m and 130m which measure the 3D wind vector. Wind vanes are installed at 126m, 80m and 21m. The direction of the booms of the mast is 160° for the left booms and 340 ° for the booms to the right (see Figure 4).

The GPS location of the meteorological mast is (LAT 51.962997°, LON 4.005338°)

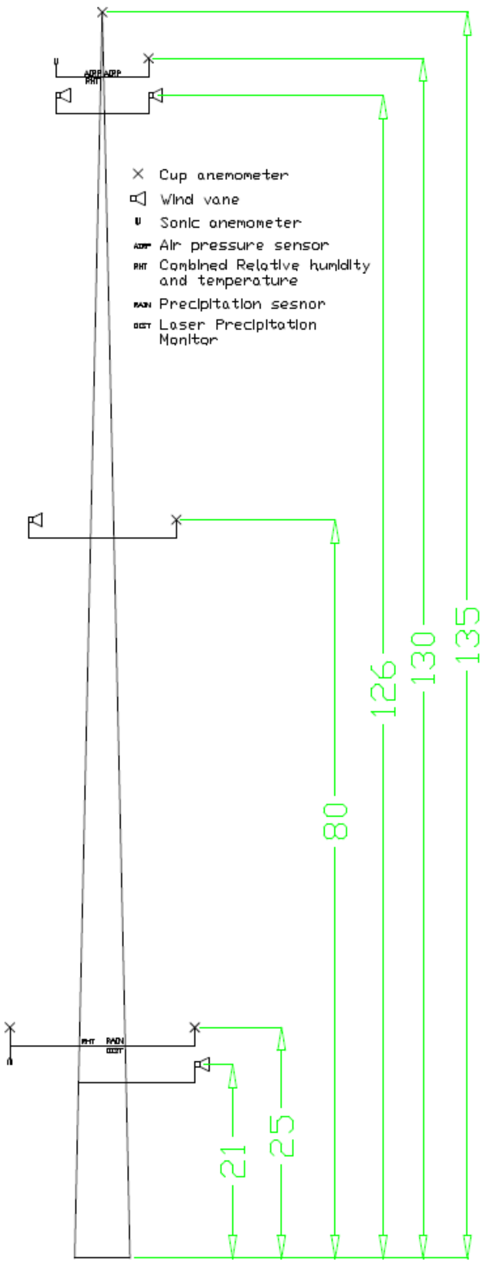

Figure 4 Meteorological mast heights and sensor layout

2.4 Measurement campaign

A two week measurement campaign is carried out from the 26th of September 2019 until the 10th of October 2019. In this period the LiDAR has measured with the scan pattern configuration defined in Table 1. The scanning patterns are repeated continuously. A detailed table with actual input parameters for this configuration in the WLS-200S can be found in Appendix A.

Table 1 Scanning patterns (looped)

Goal	Scan type	Azimuth (degree)	Elevation (degree)
Mast validation (3 heights)	PPI (double)	285..315 & 315..285	5.8, 18.2, 29.3
Free stream vertical	RHI	267	0..90
In between terminal	PPI	267..218 & 218..267	1.25, 2.6, 4.7, 24.7
In between terminal vertical	RHI	218	0..90

With respect to the validation of the scanning LiDAR with the meteorological mast we note that the mast is at 300 degrees from the LiDAR at about 270m. The elevation angles in table 1 are chosen such to match the three measurement heights of the mast. Furthermore, we note that the scanning LiDAR is programmed such that it scans in a +/- 15 degrees azimuth sector around the mast. The logic is that this sector facilitates the application of the wind speed reconstruction algorithm.

To assess the winds coming from sea to land, we determine the free stream sector according to the international IEC 61400-12-1 standard for power performance assessments [8], being from 234 degrees - 267 degrees. We extend this sector in southwest direction up to 218 degrees and in that configuration the scanning LiDAR measures exactly in between the terminals APM (southeast) and RWG (northwest). At both ends of the entire scan range from 218 degrees to 267 degrees there is a vertical (RHI) scan: at 267 degrees in the free stream and at 218 degrees in between the terminals.

For the free stream sector the heights of interest correspond the rotor of the GE Haliade X prototype turbine, i.e. a lower tip height of 25m, a hub height of 135m and a higher tip height of 245m, and the distances of interest are from 1.5D (=330m) to an extended reach of 6km. This results in the following elevations: 24.7 degrees (hub height at 1.5D; near wind field), 4.7 degrees (full rotor span between 1.5D and 3300m; intermediate wind field) and 2,6 degrees (full rotor span between 612m to 6km; far wind field).

For the wind fields around the terminals, we assume the container ships to be around 50m high at a distance in between 900m and 1800m from the LiDAR. This results in the following elevations: 1.25 degrees (20m-39m high; lower part of container ship), 2.6 degrees (37m-55m high, top part of container ship) and 4.7 degrees (66m-133m; wind fields above the container ships).

3 Scanning LiDAR validation

The first step in performing ECN.TNO's method for statistical reconstruction of wind fields [4] is to apply a Gaussian Process-based machine learning model to generate a "Virtual Lidar". This model infers what the LiDAR would have measured if the beam had been pointed anywhere in space and time.

The capabilities of statistical inference are limited by the quality and density of input data measured by the LiDAR. Therefore in the first sub-section below the scan patterns and data recovery from the LiDAR are described, with reference to the information they provide in different regions of the Rotterdam harbour.

This is followed by a validation of the Virtual Lidar modelling, by outputting a 1Hz radial wind speed prediction at the exact location of the sonic anemometer, and performing a direct comparison. This mimics the tests undertaken in [5]. Note that this is not a validation of the scanning LiDAR measurements themselves, but a validation of the scanning LiDAR measurements after post-processing, i.e. the Virtual Lidar. Their accuracy has been validated many times in previous industry-wide studies. As an example, see for instance the direct validation of a nacelle LiDAR of the same manufacturer in [9].

3.1 LiDAR measurements

The scan patterns described in section 2.4 are depicted in Figure 5. Measurement data between 100m and 7000m are returned, particularly in the southwest region, across Rotterdam harbour.

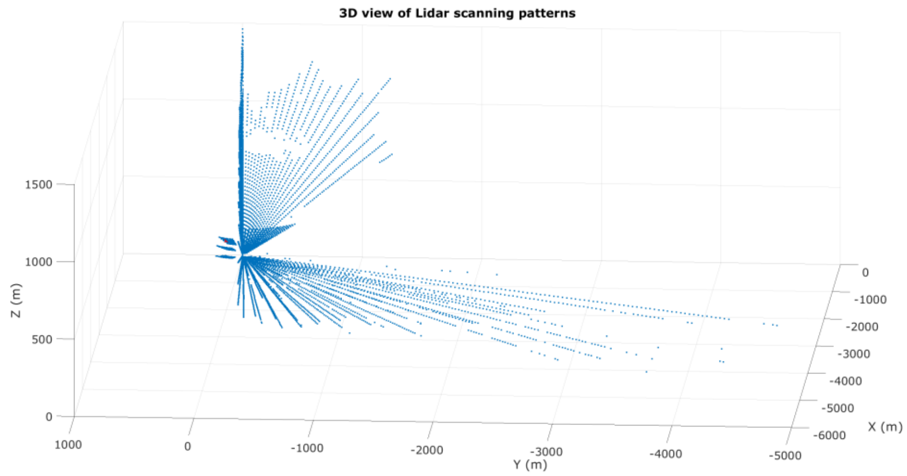

Figure 5 3D plot of example data from one iteration of all scanning patterns. Positive Y direction indicates North and positive X direction indicates East.

Note also the set of scans with a short range and higher elevation to the northwest, which cover the meteorological mast. These are separately visualized in Figure 6.

It can be seen that the inference method will be required to perform significant work, since the sonic anemometer's location is only close to a few of the points on the highest scan.

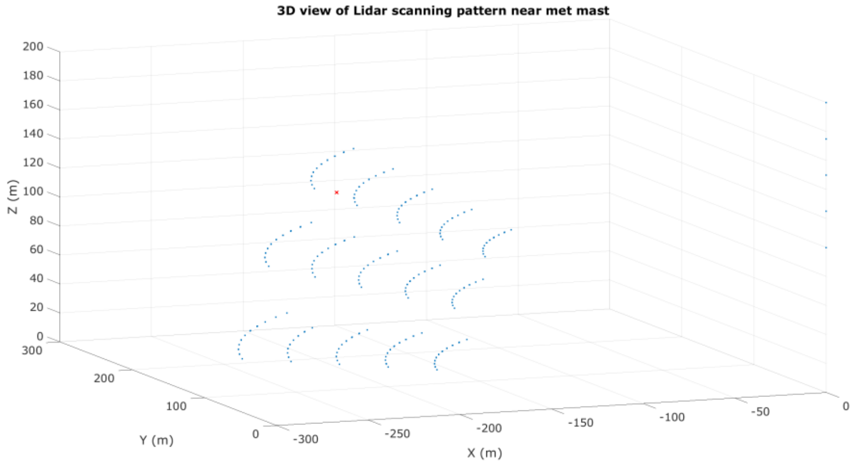

Figure 6 3D plot of example data from one iteration of the scan pattern in the northwest direction, with the sonic anemometer marked as a red cross.

Further, it is clear that by choosing to scan in many locations with different scan patterns, that means that any one location is only measured intermittently. Figure 7 shows that the whole scanning regime takes just over 4 minutes to complete.

The height of the yellow "W" line shows the amount of information content about the vertical velocity component, in other words the elevation of the scanning LiDAR beam (as previously stated, only the component of the velocity resolved to the LiDAR beam angle is captured). The first minute is taken up with scans near the meteorological mast, and the first 20 seconds, while at a low elevation, is also necessarily at a low altitude, given little detailed information about the turbulent wind experienced by the sonic anemometer.

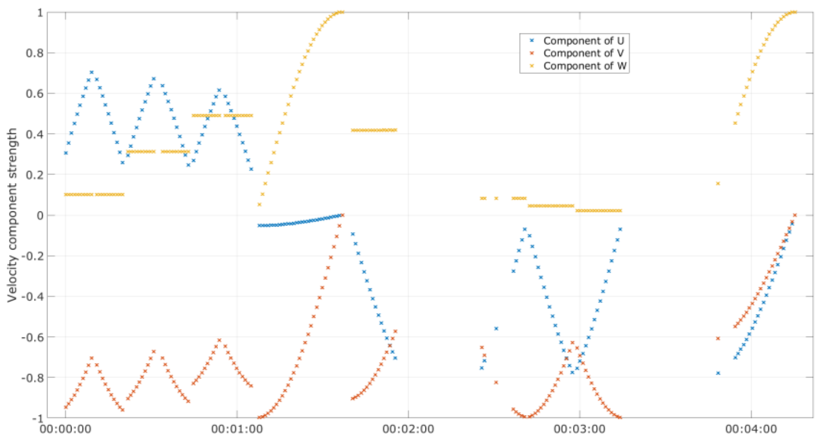

Figure 7 Example data from one iteration of all scanning patterns in time, showing the information content available for each component of the wind velocity (U: north, V: east, W: vertical)

We can now plot an example of the data available within a 50m cuboid of the meteorological mast, see Figure 8. Only those points with a yellow color will provide much information about the detailed wind conditions experienced by the sonic anemometer. Additionally, the radial wind speed recorded is of course affected by the angle of the LiDAR beam, and so while the closeness of the data to the black line ($v_r = \underline{v} \cdot \underline{\hat{b}}$) is promising, we cannot directly compare them.

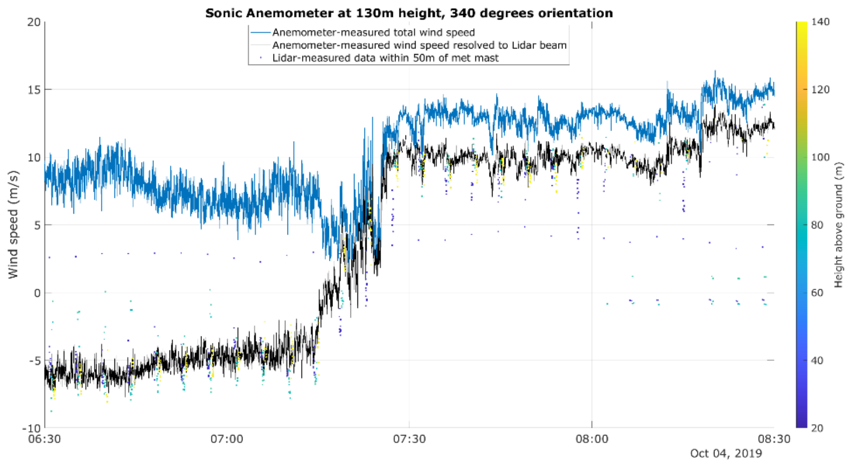

Figure 8 A two hour period during the campaign, showing the sonic anemometer-measured total wind speed (blue line), the wind velocity resolved to the LiDAR beam direction (black), and scanning LiDAR measurements (coloured dots) within a 50m zone around the meteorological mast. The colours of the LiDAR measurement points indicate height.

The entire campaign data set is now shown in the same way in Figure 9. At this scale, the yellow (quality controlled) LiDAR data points are generally well-aligned with the expected black line.

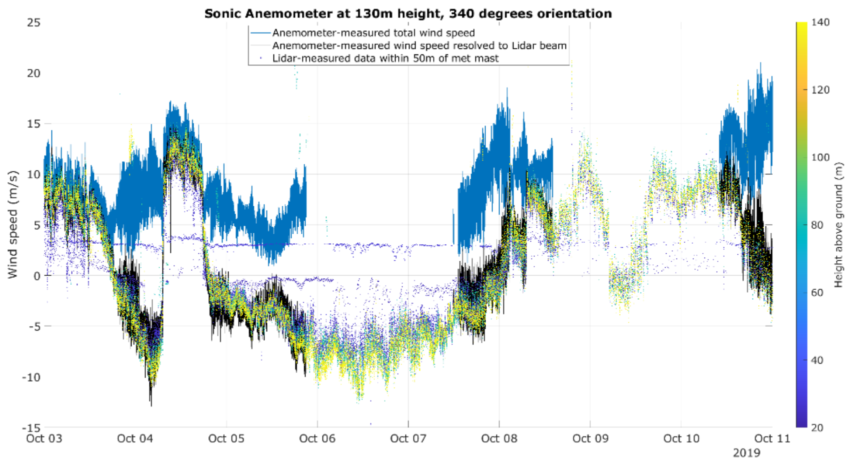

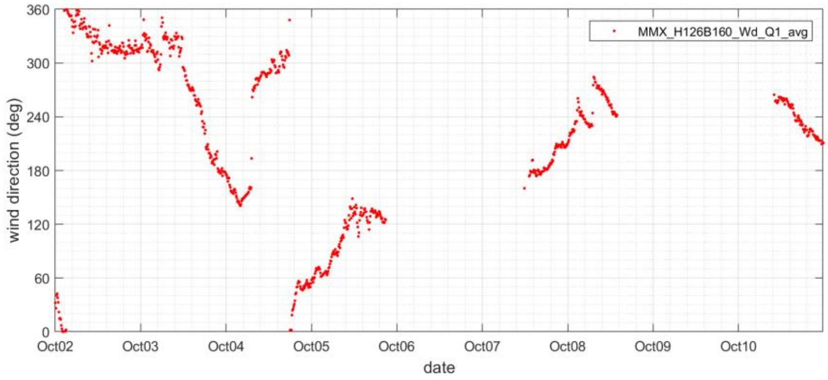

Figure 9 The upper plot shows for the entire campaign period the sonic anemometer-measured total wind speed (blue line), the wind velocity resolved to the LiDAR beam direction (black), and scanning LiDAR measurements (coloured dots) within a 50m zone around the meteorological mast. The colours of the LiDAR measurement points indicate height. The lower plot shows for the entire campaign period the wind direction as measured with a wind vane at 126m installed at the 160 degrees boom.

In conclusion, very little data is available to drive a detailed reconstruction of the wind speed experienced by the sonic anemometer, spatially and temporally. We expect the Virtual Lidar to ignore data which is not close to the point of interest, particularly the two sets of low altitude data with radial wind speeds around -0.5 and 3.5m/s. At times when useful information is not available, the Virtual Lidar will just predict using the slowly-varying average wind velocity determined from other measurements (which may be more than 1km away).

3.2 Virtual Lidar validation

The main time period from midnight on 3rd October to 21:00 on 5th October is used, when the sonic anemometer data are available. A scatter plot of the data at 1Hz is presented in Figure 10, using the mean wind speed estimate from the Virtual Lidar.

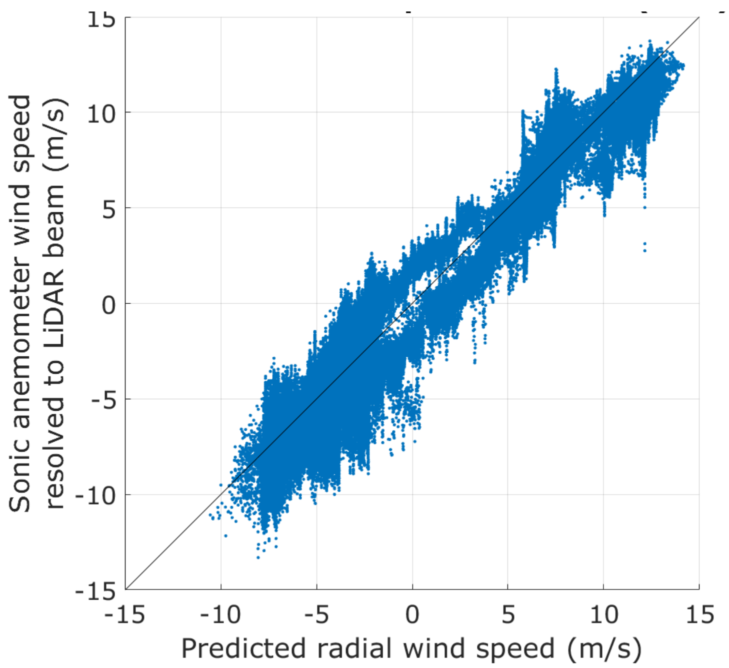

Figure 10 Scatter plot of sonic anemometer measurements, resampled at 1Hz and resolved to the LiDAR beam angle, versus predictions from the Virtual Lidar.

Over this three day period, the bias, calculated as:

$$\mu = \frac{\sum_{i=1}^{n} V_{r,pred}(t_i) - V_{r,anem}(t_i)}{n}$$

lies at 0.28 m/s.

The standard deviation of the difference between prediction and anemometer data:

$$SD = \sqrt{\frac{1}{n-1}\sum_{i=1}^{n}\left|V_{r,pred}(t_i) - V_{r,anem}(t_i) - \mu\right|^2}$$

is calculated to be 1.54 m/s.

In the previous study [5], where a more focused scan pattern was used around a meteorological mast, a scatter of 0.55-0.90m/s was achieved, depending on width and speed of the scan pattern. Now, we obtain a significant, if unsurprising, increase.

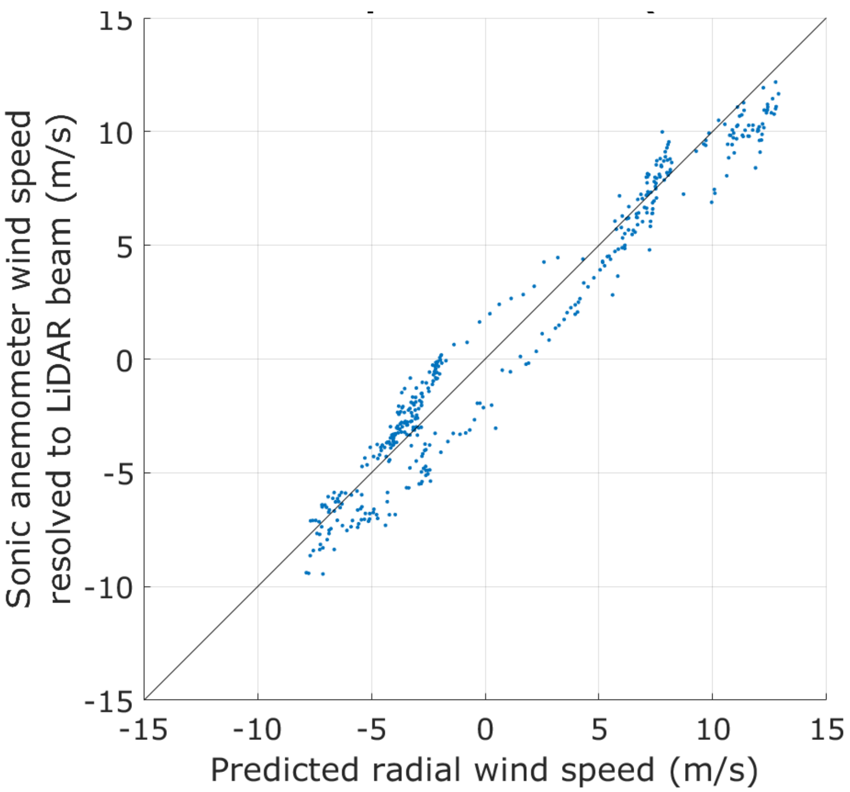

Figure 11 Scatter plot of sonic anemometer measurements, resolved to the LiDAR beam angle, versus predictions from the Virtual Lidar; both averaged to 10 minutes.

Now, averaging both data sets to 10-minutes provides the plot in Figure 11. A bias of 0.27 m/s remains while the standard deviation reduces to 1.32 m/s.

4 Wind field reconstruction

The Virtual Lidar can also be used to output instantaneous radial speeds at multiple locations at the same time. These come as Normal Distributions (mean and uncertainty). The uncertainty can then be used when combining multiple locations together to estimate the wind velocity, or as a filter, to remove points which have not had recent measurement.

4.1 Instantaneous radial wind speed maps

Radial wind speeds were output across the Rotterdam harbour at 50m height over a 3km by 3km area with 10m horizontal resolution, for specifically-chosen times when the scanning LiDAR was active in the area.

Two examples are shown in Figure 12 and Figure 13, where the plots are overlaid on Google Earth. Overlaid images such as these allow for a qualitative analysis of the wind field. However, it has to be kept in mind that the satellite image used for these visualizations is not taken at the exact time when the wind field is predicted.

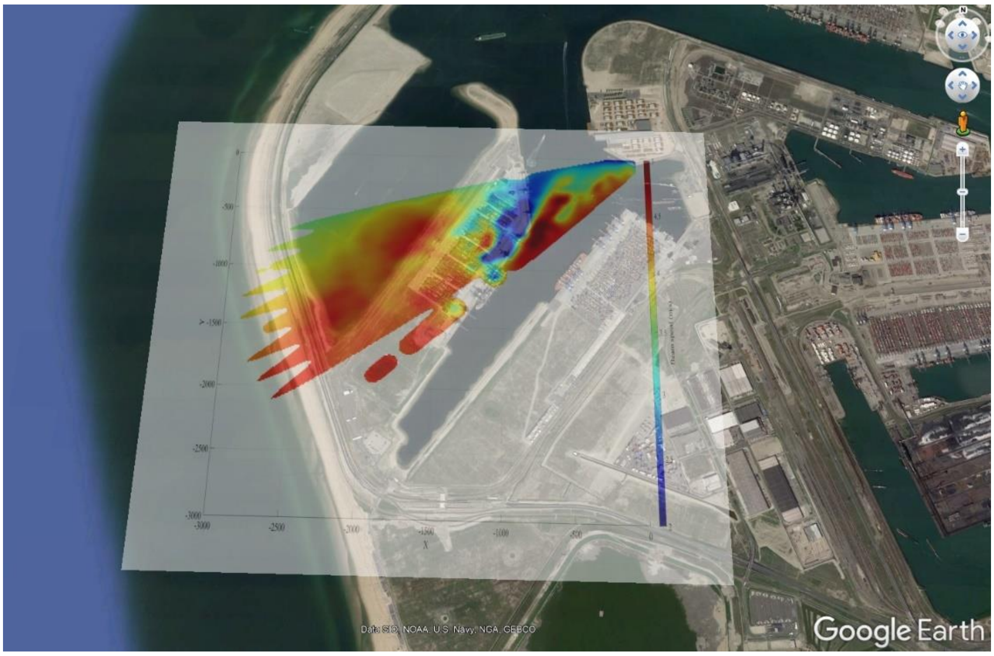

Figure 12 Radial wind speed at 50m height on 3rd of October, 18:20:22. The wind direction measured by the meteorological mast wind vane at this time is 205º (SSW).

The (white) gaps in both plots indicate where the uncertainty is high, due to lack of nearby data. There is a clear gap in both images behind the container loading area, where the LiDAR beam is blocked.

Looking at the wind speed predictions themselves, it is clear that - in these wind directions - there is a boundary between low wind speed at the top of the containers and in their wake, and unimpeded higher wind flow over the water to the east and low-lying land to the west.

Some detailed flow features appear visible around the docked vessel, however, it would need to be confirmed whether a vessel was in reality present at that time.

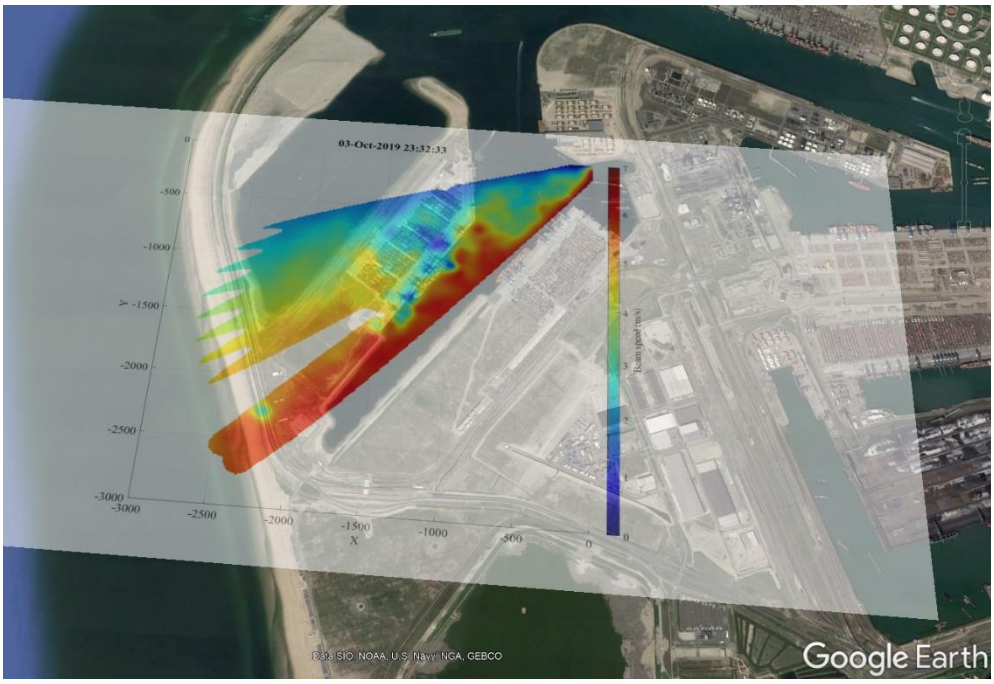

Figure 13 Radial wind speed at 50m height on 3rd of October, 23:32:33. The wind direction measured by the meteorological mast wind vane at this time is 161º (SSE).

4.2 Ten minute average wind fields

Conversion from radial wind speeds to wind velocities requires, as previous stated, a way to reverse the Cyclops equation:

$$v_r = -\begin{pmatrix} \sin\beta\sin\alpha \\ \cos\beta\sin\alpha \\ \cos\alpha \end{pmatrix}^T \cdot \begin{pmatrix} v_x \\ v_y \\ v_z \end{pmatrix}$$

where α is the angle to the vertical and β is the angle to north. v_x, v_y and v_z are often also labelled U, V and W respectively.

This is performed in this study via Maximum Likelihood Estimation, using data within half of the desired resolution horizontally and vertically, and 10 seconds temporally. Only data which pass the filter on uncertainty are used (see section 4.1). All the resulting 10-second wind velocity maps in a 10-minute period are then averaged together to obtain a single wind field. Since the filtering results in many locations with no wind velocity estimate (given this set of scan patterns which take 4 minutes to complete) results are presented here with blank spaces linearly interpolated.

Figure 14 and Figure 15 show examples of wind conditions coming respectively from the west and the southeast, output at 50m X and Y resolution and 20m Z resolution. The effects of the tall structures can be clearly seen: wake in the lee of the containers at higher heights; speed-up effects and turbulence around containers at low heights; and an alignment of the flow with the pathways running through the containers. This is despite the fact that the LiDAR's beam angle, perpendicular to the flow, implies that very little of the bulk wind speed can be measured.

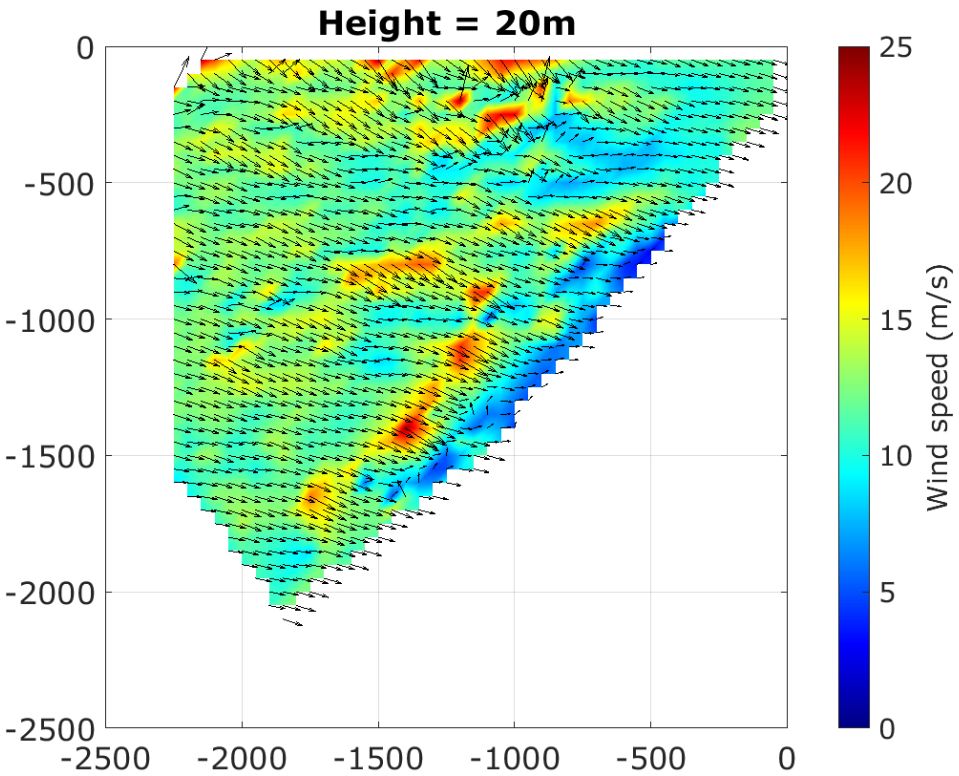
Height = 20m
0
-500
-1000
-1500
-2000
-2500
-2500 -2000 -1500 -1000 -500 0
25
20
15
10
5
0
Wind speed (m/s)

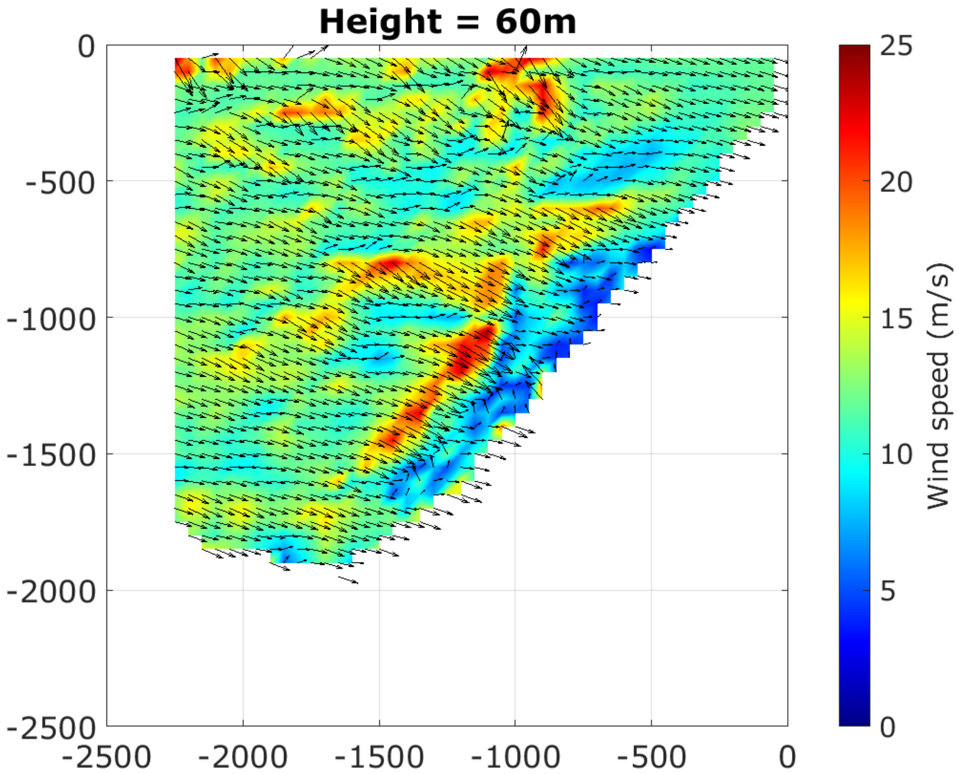
Height = 60m
0
-500
-1000
-1500
-2000
-2500
-2500 -2000 -1500 -1000 -500 0
25
20
15
10
5
0
Wind speed (m/s)

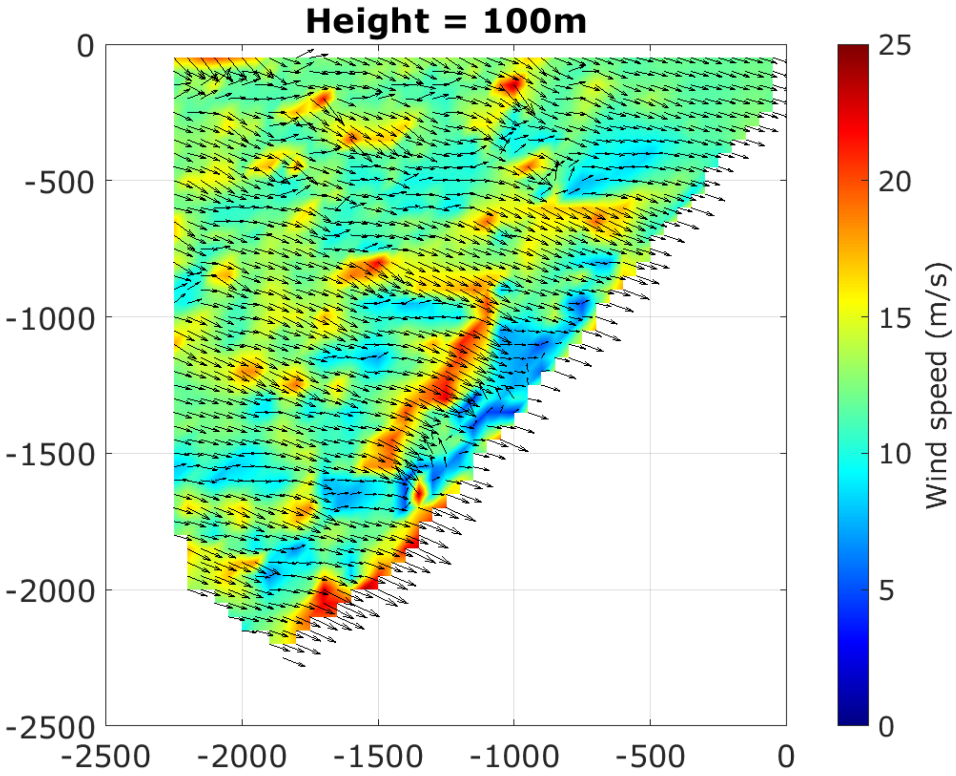

Figure 14 10-minute averaged wind fields, output at three heights (top to bottom: 20m, 60m, 100m) for 4th October 2019 14:30–14:40. The colours and arrows indicate the horizontal wind speed and direction

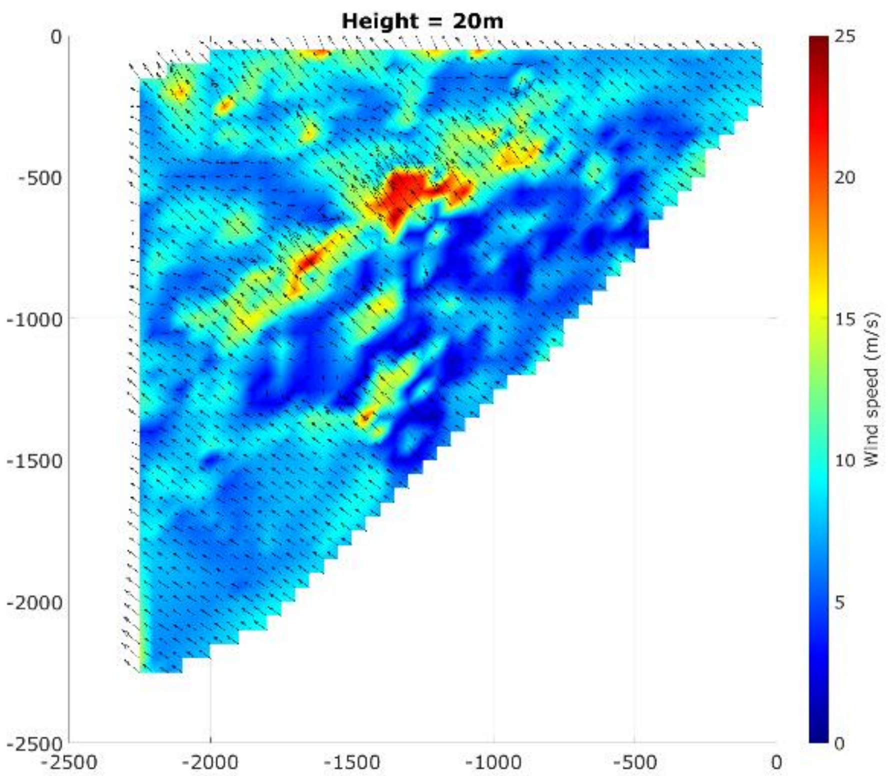

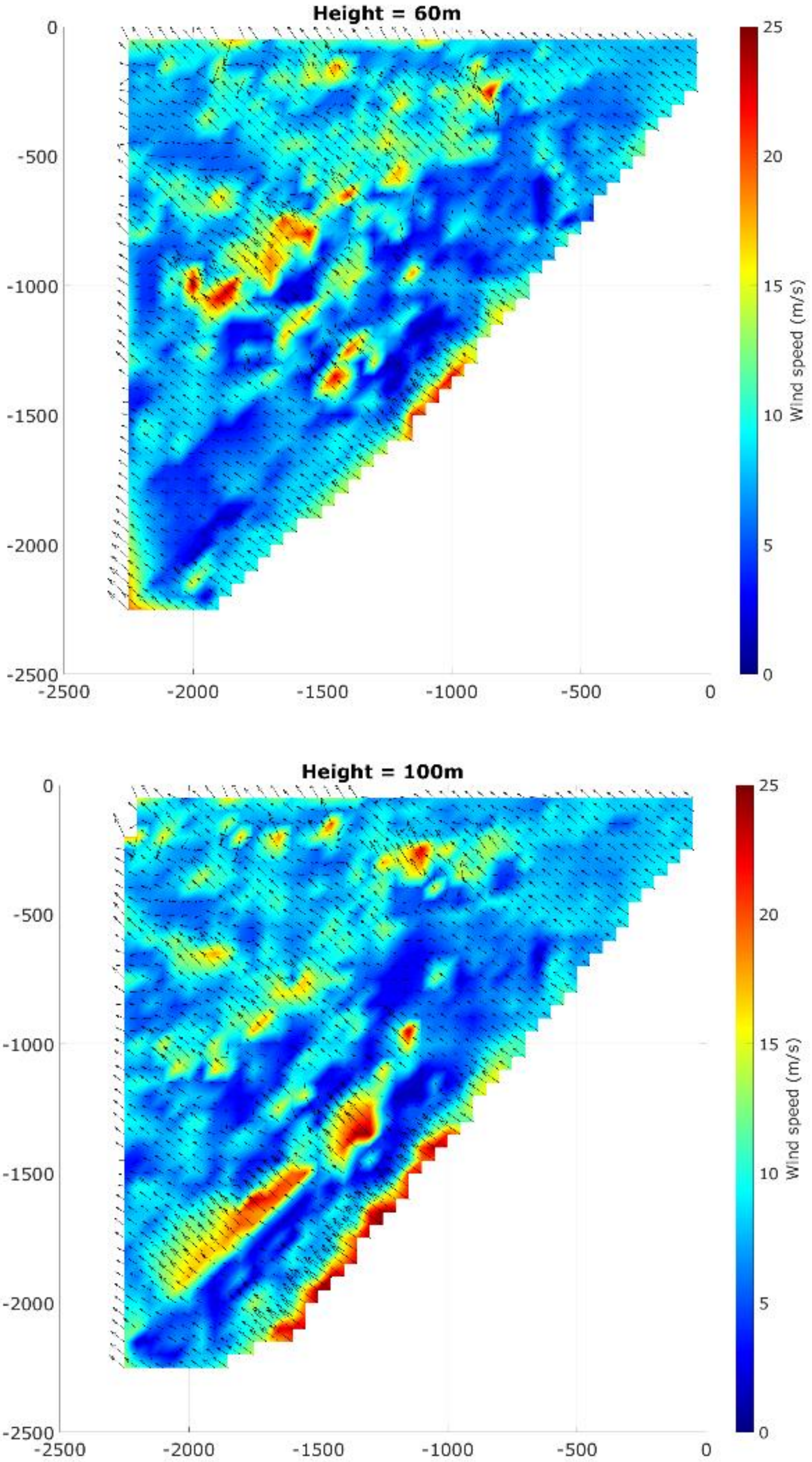

Figure 15 10-minute averaged wind fields, output at three heights (top to bottom: 20m, 60m, 100m) for 5th October 2019 20:30–20:40. The colours and arrows indicate the horizontal wind speed and direction.

From the above figures (Figure 12 to Figure 15) no clear conclusions can be drawn on how the wind approaches from sea to land. Although, the winds in the figures are not directly from the undisturbed sector, the flow over the terrain can be addressed. This is relevant for the undisturbed wind assumption in power performance testing [8]. Particularly, Figure 12 and Figure 14 give indications in that respect and we see that terrain influences are still visible at 100m. However, at this moment there is no indication that influences are such that undisturbed wind condition assumptions need to be revised. It would also require a more detailed and focused study to make conclusive statements in this respect.

5 Conclusions and Recommendations

A two-week campaign of scanning LiDAR measurements in Rotterdam harbour has been completed. The data collected have been used in a machine learning model developed by ECN.TNO to demonstrate reconstruction of wind fields across the harbour. The intention was to be able to measure wind flows from sea to land and around container ships while docked, to inform load calculations.

Validation of the machine learning method in these complex conditions was first conducted by reconstructing the measurements obtained at a sonic anemometer located on a nearby meteorological mast. This task was made significantly more difficult by the complex scanning pattern chosen, which aimed to achieve several goals. As a result, measurements within a reasonable distance of the sonic anemometer were only available intermittently, which limits the possibilities for effective statistical inference. The validation results for 10-minute average wind speeds showed a bias of +0.27 m/s and a high standard deviation of 1.32 m/s.

The location of the LiDAR also complicated investigation of flow patterns perpendicular to the container vessel (oriented SW-NE), as the LiDAR does not capture any wind flowing perpendicular to its beam direction. Despite this, interesting instantaneous and 10-minute average wind flow fields were reproduced.

With respect to how the wind approaches from sea to land in the free stream (undisturbed wind conditions), no clear conclusions can be drawn. Nevertheless, the study clearly shows that terrain influences are still visible at 100m relevant for undisturbed wind condition assumptions in for instance power performance testing. However, at this moment there is no indication that influences are such that undisturbed wind condition assumptions need to be revised.

With respect to the wind field reconstructed flow fields around and in between container ships, the effects of the tall structures can be clearly seen in the results: wake in the lee of the containers at higher heights; speed-up effects and turbulence around containers at low heights; and an alignment of the flow with the pathways running through the containers.

For an extended future study, significantly improved results can be obtained by:

1. Positioning the LiDAR with:
    - an unobstructed view of the containers,
    - such a scan area where the wind is flowing along the LiDAR beam directions.
2. Avoiding changing range gates in the scan pattern sequence as this takes significant time. We recommend to choose a single PPI scanning mode at a small number of heights, such that a good balance is obtained between the cross-sectional area covered and minimising the time between return scans of the same location. In this sense a single scan should easily be completed within 30 seconds.

6 References

[1] Declaration of Intend on ‘WindScanner.nl’, ECN, MARIN, KNMI, NLR, WUR, December 2018.

[2] Leosphere WindCube 200S Brochure, http://www.leosphere.com/products/3d-scanning/windcube-100s200s400s-turbulence-wind-lida’

[3] TKI Wind op Zee ‘Demonstrator GE Haliade X – 12MW offshore wind turbine project’, https://projecten.topsectorenergie.nl/projecten/demonstrator-ge-haliade-x-12-mw-offshore-windturbine-00031437

[4] C. Stock-Williams, et al, ‘’Wind field reconstruction from lidar measurements at high-frequency using machine learning”, *J. Phys.: Conf. Ser.* **1102** 012003, 2018

[5] C. Stock-Williams, ‘Reconstruction of Wind Fields from Scanning Lidar’, DOI 10.5281/zenodo.3360261, 2019

[6] H. vd Boom, Project proposal: Wind Loads And Securing Ships ‘WINDLASS’ JIP pilot project; IC_D0492018_RH_0043, project lead MARIN, 2018

[7] J.W. Wagenaar, ‘Scanning LiDAR test at the GE Haliade X wind turbine on the Sif site’, project plan 060.39123, 2019

[8] IEC, ‘Wind energy generation systems – Part 12-1: Power performance measurements of electricity producing wind turbines’, IEC 61400-12-1 Edition 2, March 2017.

[9] J.W. Wagenaar, et al, ‘Wind Iris nacelle LiDAR calibration at ECN test site’, ECN-X—16-116, 2016.

A WLS-200s configuration parameters

		repetitions	azymuth			elevation			sample time	distance			range gate
category	scan name	(#)	start(deg)	stop(deg)	speed(deg/s)	start(deg)	stop(deg)	speed(deg/s)	(ms)	start(m)	number(#)	step size(m)	(m)
validation to mast	PPI_SIF_MMX_el5.8_sp1_direct	1	285	315	3	5.8			1000	200	5	25	25
	PPI_SIF_MMX_el5.8_sp1_indirect	1	315	285	3	5.8			1000	200	5	25	25
	PPI_SIF_MMX_el18.2_sp1_direct	1	285	315	3	18.2			1000	200	5	25	25
	PPI_SIF_MMX_el18.2_sp1_indirect	1	315	285	3	18.2			1000	200	5	25	25
	PPI_SIF_MMX_el29.3_sp1_direct	1	285	315	3	29.3			1000	200	5	25	25
	PPI_SIF_MMX_el29.3_sp1_indirect	1	315	285	3	29.3			1000	200	5	25	25
free stream	RHI_SIF_az267_direct	1	267			0	90	3	1000	100	100	25	25
free stream + in between terminals	PPI_SIF_terminal_el24.7_sp1_indirect	1	267	218	3	24.7			1000	50	25	25	25
	PPI_SIF_terminal_el4.7_sp1_direct	1	218	267	3	4.7			1000	100	70	50	50
	PPI_SIF_terminal_el2.6_sp1_indirect	1	267	218	3	2.6			1000	100	140	50	50
	PPI_SIF_terminal_el1.25_sp1_direct	1	218	267	3	1.25			1000	100	70	50	50
in between terminals	RHI_SIF_az218_direct	1	218			0	90	3	1000	100	100	25	25